Novel Robust Watermarking Technique in Dithering Halftone Images

Soo-Chang Pei, *Fellow, IEEE*, Jing-Ming Guo, and Hua Lee, *Fellow, IEEE*

***Abstract*—In this letter, we present a novel robust method for embedding watermarks into dithered halftone images. The method is named paired sub-image matching ordered dithering (PSMOD), of which the decoder is provided with *a priori* information of the original watermark. The method utilizes the bit and sub-subimage interleaving preprocesses. The experiments show that the technique is sufficiently robust to guard against the cropping, tampering, and printed-and-scanned degradation processes, in either B/W or color dithered images. This technique is also sufficiently flexible for various levels of embedded capacities.**

***Index Terms*—Bit-interleaving, error diffusion, halftone, ordered dither.**

I. Introduction

DIGITAL halftoning is converting multitone images into two-tone format, which is commonly used in computer printouts, books, newspapers, and magazines [1]. When viewed at a proper distance, halftone images resemble the original due to the lowpass nature of the human visual systems. In practice, the two most common types of halftoning techniques are ordered dithering and error diffusion [1], [2]. Between these two, ordered dithering is more efficient and offers good visual quality.

Several methods for watermarking in halftone images have also been developed. These techniques are regularly applied to the printing of security documents, such as ID cards, currencies, and confidential documents, to prevent illegal duplication and forgery. These methods can be divided into three categories.

The first category involves low computational complexity using ordered dithering but nonflexible embedded capacity watermarking. These methods use different dither cells to create a threshold pattern in the halftoning process, and each dither cell represents the corresponding information bit in watermark [3], [4].

The second category has higher computational complexity for direct binary search and error diffusion. These methods are capable of obtaining a higher quality of embedded image watermarking, which includes obtaining good visual quality as well as good watermark detection with joined direct binary search (DBS) halftoning and spread spectrum watermarking algorithms [5]. There are some applications of vector quantization (VQ) to embedding watermarks into the most or least significant bit (MSB/LSB) of error diffusion images. The benefits of this approach are that a low bit-depth halftone for printing or progressive transmission can be achieved by masking one or more bits off of the higher bit-depth image [6]. Adopting modified data hiding error diffusion (MDHED) to embed data into error diffusion images, where the method is effectively to hide a relative amount of data with good quality halftone images, and the amount of hidden data is easy to control [7].

The third category involves low computational complexity. However, the decoded result is an approximation of the original watermark. This is to embed a watermark into dithering images by using a pair of conjugate halftone screens. Fourier analysis can be utilized to determine the periodicity of the embedded printed-and-scanned image, and then, the embedded watermark can be obtained by the superposition of correlated portions of the image [8].

In this letter, we propose a robust watermarking techniques by embedding the watermark into a dithered image after the preprocess of bit-interleaving and sub-image-interleaving [9]. The method is capable of achieving good visual quality and flexibility for various embedded capacities while maintaining low computational complexity of ordered dithering using the threshold process.

II. Bit-Interleaving

Halftoning screens are designed for various specific purposes. As an example, Fig. 1(a) shows a dispersed-dot dithering screen [1]. Generally speaking, the choice of dispersed-dot screen and clustered-dot screen is mainly based on printing process problems. Clustered-dot screens can hide artifacts commonly seen in laser printing, such as dot gain effect. However, the image quality is lower because of the lack of spatial resolution. On the other hand, dispersed-dot screens provide higher image quality. However, they exacerbate process artifacts of laser printing and are, therefore, mainly used in inkjet printers. To illustrate the algorithm of ordered dithering, we can define the halftone screen as $M \times N$ matrix array. Each pixel $x_{i,j}$ in the original gray-level image is mapped to a halftone screen value $\mathrm{HS}_{i \bmod M, j \bmod N}$. The dithered output $b_{i,j}$ is determined as

$$b_{i,j} = \begin{cases} 255 \text{ (white)}, & \text{if } x_{i,j} \geq \mathrm{HS}_{i \bmod M, j \bmod N} \\ 0 \text{ (black)}, & \text{if } x_{i,j} < \mathrm{HS}_{i \bmod M, j \bmod N}. \end{cases} \quad (1)$$

Manuscript received February 16, 2004; revised June 26, 2004. This work was supported by the National Science Council, China, under Contracts NSC93-2752-E-002-006-PAE and NSC 93-2219-E-002-004. The associate editor coordinating the review of this manuscript and approving it for publication was Prof. Mark Hasegawa-Johnson.

S.-C. Pei is with the Department of Electrical Engineering, National Taiwan University, Taipei, Taiwan 10617, R.O.C. (e-mail: pei@cc.ee.ntu.edu.tw).

J.-M. Guo is with the Department of Electrical Engineering, National Taiwan University, Taipei, Taiwan 10617, R.O.C. and also with the Department of Electronic Engineering, Jin Wen Institute of Technology, Taipei, Taiwan 231, R.O.C. (e-mail: jmguo@seed.net.tw).

H. Lee is with the Department of Electrical and Computer Engineering, University of California, Santa Barbara, CA 93106-9560 USA (e-mail: hualee@ece.ucsb.edu).

Digital Object Identifier 10.1109/LSP.2004.842295

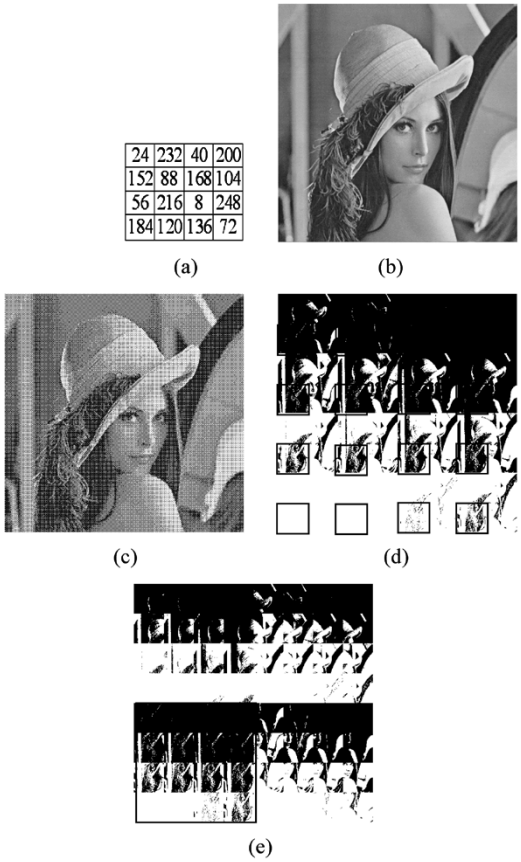

Fig. 1. (a) 4×4 halftone screen. (b) Original 512×512 gray-scaled Lena image. (c) Dithered image (PSNR $= 32.29$ dB). (d) After bit-interleaving. (e) After image dividing and SSI-interleaving processes. (All printed at 300 dpi).

Fig. 1(c) is the dithered Lena image of the original gray-scale image, shown as Fig. 1(b), processed with a halftone screen given as Fig. 1(a). The bit-interleaving procedure extracts and gathers all the pixels corresponding to the same threshold value in Fig. 1(a) to form the final image, shown as Fig. 1(d). In this case, the final image is composed of 16 subimages.

III. Error Criterion

Let the size of the original image be $P \times Q$. The error criterion is defined as below.

$$\text{PSNR} = \frac{P \times Q \times 255^2}{\sum_{i=1}^{P} \sum_{j=1}^{Q} \left[x_{i,j} - \sum_{m,n \in R} \sum w_{m,n} b_{i+m,j+n} \right]^2} \tag{2}$$

where R is the support region of the human visual coefficients, and $w_{m,n}$ is the human visual coefficient at (m, n), which can be obtained by psychophysical experiments [10]. The other method to obtain w is to use a training set of both pairs of gray-level images and good halftone results of them, such as using error diffusion or ordered dithering to produce the set. Here, we use Least-Mean-Square (LMS) to derive w as described below.

$$e_{i,j}^2 = \left(x_{i,j} - \sum_{m,n \in R} \sum w_{m,n} b_{i+m,j+n} \right)^2 \tag{3}$$

$$w_{m,n}^{(k+1)} = w_{m,n}^{k} + \mu e_{i,j} b_{i+m,j+n}, \tag{4}$$

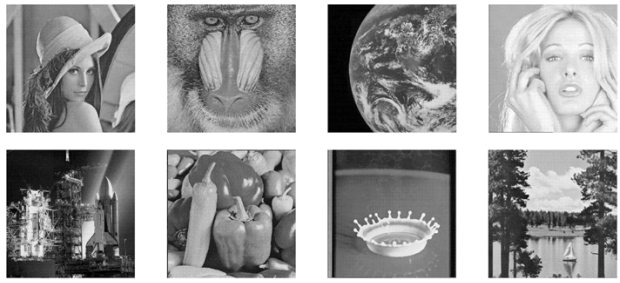

Fig. 2. Thumbnail of eight tested images. Left to right: Lena, Mandrill, Earth, Tiffany, Shuttle, Peppers, Milk, and Lake.

where $w_{i,j,\text{opt}}$ is the optimum LMS coefficient, $e_{i,j}^2$ is the MSE between $x_{i,j}$, and $\widehat{x}_{i,j}$; μ is the adjusting parameter used to control the convergent speed of the LMS optimum procedure, with the value set to 10^{-5}. Equation (4) is implemented on a pixel-by-pixel basis. There are eight 512×512 training images used in the training process: Lena, Mandrill, Earth, Tiffany, Shuttle, Peppers, Milk, and Lake images. The thumbnails of these images are shown in Fig. 2. The Bayer-5 dispersed-dot halftone screen and Floyd error diffusion are used to produce the corresponding halftone training results [1]. In total, five passes should be done with these eight trained images before the algorithm converges. As given in (3), the halftone image cooperates with the obtained coefficients and can approach to the original gray level image. The LMS-trained coefficients play a role similar to the lowpass characteristics of human eyes. With this criterion, the quality of the original dithered image shown in Fig. 1(c) is measured at 32.29 dB.

IV. Watermarking in Dithered Images

A. Paired Sub-Image Matching Ordered Dithering (PSMOD)

Let $x_{i,j,1}, x_{i,j,2}, \ldots, x_{i,j,m}$ be the subimage sequence after bit-interleaving, where $\mathrm{m} = n^2$. We pick $\mathrm{m} = 64$ and $\mathrm{n} = 8$ for this example. From the left to right, bottom to top, we pair the subimages as $(x_{i,j,k}, x_{i,j,k+1}), \mathrm{k} = 2\mathrm{t} + 1$, for $\mathrm{t} = 0, 1, \ldots, 31$, to produce 32 pairs of subimages. For each pair, we assume $x_{i,j,k+1}$ has more black pixels than $x_{i,j,k}$. We then define $x_{i,j,k+1}$ as the black subimage and $x_{i,j,k}$ as the white subimage. The original order $(x_{i,j,k}, x_{i,j,k+1})$ represents a white pixel in watermark, and $(x_{i,j,k+1}, x_{i,j,k})$ represents a black pixel. In the decoder, the watermark is extracted by an AND operation between the watermarked image and the original watermark. Since the watermark is extracted by the "AND" operation, it is necessary to eliminate the Non-Increased black pixel Pairs (NIPs) in the relative position only where the watermark has a black pixel.

Subsequently, we focus on the improvement of the embedded capacity by the PSMOD method. First, we enlarge the halftone screen from 8×8 to 16×16, so that, after bit-interleaving, 128 bits can be used for embedding. In the watermarking scheme, the accurate decoding result is based on the assumption that, in the pair of subimages, $(x_{i,j,k}, x_{i,j,k+1}), x_{i,j,k+1}$ contains more black pixels than $x_{i,j,k}$. If the likelihood of $x_{i,j,k}$ has more black pixels than $x_{i,j,k+1}$, the erroneous decoding rate increases as well. The statistics of NIP are shown in Table I. For the experiments, eight images, as described in Section III, are utilized

TABLE I
STATISTICAL NUMBER OF NONINCREASED BLACK PIXEL PAIRS (NIP), ADDITIVE PSEUDO PIXELS, AND DECODING ERROR RATES

Size of halftone screen	4×4	4×4	4×4	4×4	8×8	8×8	8×8	16×16
Dividing number of every sub-image	1	4	16	64	1	4	16	1
embedded watermark bits	8	32	128	512	32	128	512	128
Average number of NIP	1	5	35	230	6	38	254	56
Number of additive psudo pixels	1	18	68	327	21	130	575	320
Decoding error rate (%)(without pseudo pixels)	5.3	7.8	13.7	22.5	9.1	15	24.8	21.7
PSNR (dB)	31.35	31.33	31.24	30.79	30.59	30.41	29.58	30.2

for testing. Table I indicates that the erroneous decoding rate of every embedded bit increases rapidly from 9.1 to 21.7% as the size of halftone screen increases form 8×8 to 16×16.

The second method utilizes the strategy of further dividing each bit-interleaved subimage into "sub-subimage (SSI)" and then executes the "SSI-interleaving" over again. An example of the image dividing and SSI-interleaving process is shown in Fig. 1. In Fig. 1(d), each subimage is further divided into four SSIs, and then, the 16 SSIs marked with the red squares in Fig. 1(d) are reordered into the large red square in Fig. 1(e). If we pair the SSIs in Fig. 1(e) into $(x'_{i,j,k}, x'_{i,j,k+1})$, where $\mathrm{k} = 2\mathrm{t}+1$ and $\mathrm{t} = 0, 1, \ldots, 31$ as before, $x'_{i,j,k+1}$ still normally has more black pixels than $x'_{i,j,k}$. In this way, we still can embed a watermark of 32 bits, although the size of halftone screen is fixed at 4×4.

Some observations are noteworthy.

1) For a fixed halftone screen size, the size of the embedded watermark can be increased by image dividing and SSI-interleaving. The erroneous decoding rate increases slower than directly using the larger halftone screen size.
2) The smaller of the halftone screen size and more divided SSIs result in a lower decoding error rate. However, a smaller halftone screen renders fewer gray levels of a dithering image at a viewing distance.

Finally, we examine the solution to the NIP problem. The NIP problem can be solved if we adequately increase the number of black pixels in $x_{i,j,k+1}(x'_{i,j,k+1})$ subimage or increase the number of the white pixels in $x_{i,j,k}(x'_{i,j,k})$. We name the additive black and white pixels as pseudo-pixels. Because of the low-pass characteristics of the human visual system (HVS), the best additive pseudo-pixels position is in the high-frequency region of an SSI. When an NIP occurs, we use the concept of sliding window, which only covers two pixels in an SSI. If the value of the two pixels is different, it implies a high-frequency region. If the pair of SSIs are both black or white, we can place the pseudo-pixel in any position to eliminate the NIP. The average additive pseudo-pixels number used to solve the NIP problem in eight tested images is shown in Table I. For the same size of the embedded watermark, the dithering image with more dividing requires fewer pseudo-pixels.

B. Watermark Extraction After Printed-and-Scanned Process

In the most common applications of halftoning in printing books, newspapers, and magazines, the original embedded watermarked image is often destroyed by the printed-and-scanned process, e.g., zooming, rotation, and dot gain. Extracting the original watermarks perfectly is a difficult task. In our extraction process, we put auxiliary synchronized black pixels in four corners of the embedded halftone image. The printed-and-scanned embedded image is first rerotated by Adobe Photoshop 7.0. The size of the printed-and-scanned image is usually larger than expected when the same DPI of printing and scanning are applied. The printed-and-scanned embedded image should be geometrically transformed into 512×512 before the decoding process. To solve the problem, the printed-and-scanned image is divided into 512×512 square blocks (here, we assume that the original image dimension is 512×512), and the average of the pixels within a block is thresholded to recover the original halftone image pixel (0-black or 255-white). Since the laser printer has the problem of dot gain, here, the threshold was set lower than 128 (100 in this letter) to overcome the dot-gain effect. Some points should be addressed here. In this work, we adopted an Epson AcuLaser C2000 printer and an Epson photo 700 scanner. Before the embedded halftone image is printed, the format is saved in a bitmap and sent directly to the printer. Since the format is a bitmap, the printer driver has no further halftone processing with the image.

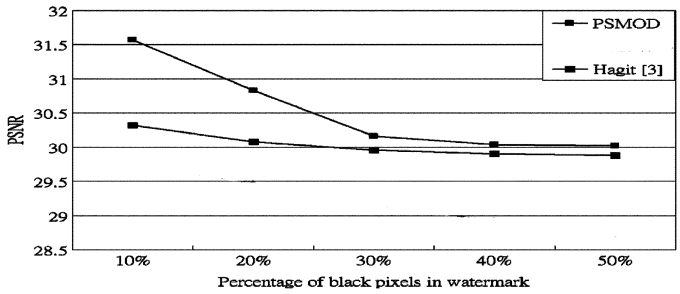

Fig. 3. PSNR versus percentage of black pixels in watermark.

In most applications, color halftone images are obtained by processing the three-color spaces (red, green, and blue) separately. Based on this concept, we can embed the same watermark in these color spaces and retrieve it by majority voting. As documented in Section IV, the experiments demonstrate a highly correct decoding rate.

V. EXPERIMENTAL RESULTS

To verify and document the performance of these techniques, we conducted a sequence of experiments. The black pixels in the watermark can cause the insertion of additional pseudopixels or SSI swapping and, consequently, degradation to the quality of the embedded image. Fig. 3 illustrates the PSNR as functions of black-pixel percentage in the watermark with pseudo-random-generated black pixels. When the percentage exceeds 50%, we

(a) (b) (c)

Fig. 4. (a) Watermark of size 64×64 is embedding into (b). (b) PSMOD embedded dithering image PSNR $=$ 31.11 dB. (c) Bit and SSI-interleaved version of (b).

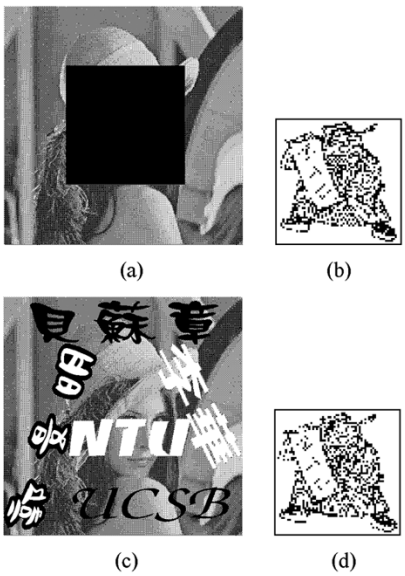

(a) (b) (c) (d)

Fig. 5. Robust watermarking testing. (b) and (d) are decoded watermarks form (a) and (c) with correct decoding rates of 95.01 and 94.62, respectively. (a) is cropped by $1/4$ portion. (c) is tampered.

can modify the algorithms by adding pseudo-pixels or SSI swapping once if white pixels appear in the watermark. The proposed PSMOD technique, even in the critical situation of 50% black pixels, can still achieve higher PSNR than Hagit's method.

Fig. 4(a) shows the original embedded watermark of sizes 64×64 and is embedded into Fig. 4(b); Fig. (c) is the SSI-interleaved result with the PSMOD technique. In Fig. 4(c), each subimage is divided into 512 SSIs (to 16 portions horizontally and to 32 portions vertically). The objective quality of Fig. 4(b) is 31.11 dB.

Subsequently, we conduct a series of experiments to demonstrate the robustness of these techniques. In Fig. 5, we try to analyze the degradation of the embedded dithered image, as shown in Fig. 4(c), due to cropping and tampering. The correct decoding rate of 95.01 is obtained with the cropping attack, and 94.62 is obtained with the tampering attack. The decoded results are shown in Fig. 5(b) and (d), respectively.

Table II shows the average correct decoding rates of the embedded dithered images with eight tested images, as shown in Fig. 2, in various configurations, including black and white and color images, as well as bitmap and scanned-and-printed images in different resolutions. Table II also shows that color images, using majority voting, as described in Section IV-C, result in greater accuracy than the black and white images. The printed-and-scanned process reproduces the embedded image at 150 dpi and scans at 150, 450, and 750, respectively. The results also show that higher scan resolution improves the accuracy of the decoding rates.

TABLE II
AVERAGE CORRECT DECODED RATES

		Bitmap	Printed-and-Scanned		
			150dpi	450dpi	750dpi
PSMOD	B&W	100	89.23	91.74	92.06
	Color	100	91.45	93.87	94.19

VI. CONCLUSION

In this letter, a novel watermarking scheme, namely PSMOD, for dithered images was presented. The technique demonstrated good recovery abilities in cropping, tampering, and printed-and-scanned distortions. In addition, it has been extended to color images and decoded, based on the concept of majority voting, and retained a high decoding rate. The watermarking scheme also provided satisfactory embedded quality and flexibility to situations of various embedded capacities. Although the technical discussions in this letter were limited to dispersed-dot dithering images, with slight modifications, it can also be generalized to clustered-dot dithering images in a similar manner.

Although the proposed technique PSMOD produces higher embedded quality and flexibility in handling different embedded capacities, its correct-decode rate is not as high as that achieved by Hagit's method [3].

REFERENCES

[1] R. Ulichney, *Digital Halftoning*. Cambridge, MA: MIT Press, 1987.
[2] J. F. Jarvis, C. N. Judice, and W. H. Ninke, "A survey of techniques for the display of continuous-tone pictures on bilevel displays," *Comput. Graph. Image Process.*, vol. 5, pp. 13–40, 1976.
[3] H. Z. Hel-Or, "Watermarking and copyright labeling of printed images," *J. Elect. Imaging*, vol. 10, no. 3, pp. 794–803, Jul. 2001.
[4] Z. Baharav and D. Shaked, "Watermarking of dither halftoned images," in *Proc. IS&T/SPIE Conf. Security Watermarking Multimedia Content*, vol. 3657, 1999, pp. 307–316.
[5] D. Kacker and J. P. Allebach, "Joint halftoning and watermarking," *IEEE Trans. Signal Process.*, vol. 51, no. 4, pp. 1054–1068, Apr. 2003.
[6] J. R. Goldschneider, E. A. Riskin, and P. W. Wong, "Embedded multilevel error diffusion," *IEEE Trans. Image Process.*, vol. 6, no. 7, pp. 956–964, Jul. 1997.
[7] M. S. Fu and O. C. Au, "Hiding data in halftone image using modified data hiding error diffusion," in *Proc. SPIE Conf. Visual Commun. Image Process.*, vol. 4067, 2000, pp. 1671–1680.
[8] S. G. Wang and K. T. Knox, "Embedding digital watermarks in halftone screens," in *Proc. SPIE Conf. Security Watermarking Multimedia Contents II*, vol. 3971, 2000, pp. 218–227.
[9] C. N. Judice, "Data reduction of dither coded images by bit interleaving," *Proc. Soc. Inf. Display*, vol. IT-17, no. 2, pp. 91–97, 1976.
[10] J. Mannos and D. Sakrison, "The effects of a visual fidelity criterion on the encoding of images," *IEEE Trans. Inf. Theory*, vol. 20, no. 4, pp. 526–536, Jul. 1974.